A Method for Estimating the Distance of Near-Ocean-Bottom Sources by Combining VLF Underwater Acoustic Field and Scholte Wave Field

Han Zhao[1], Guiqing Sun[1], Hanhao Zhu[2], Junxin Yuan[1]

1 Institute of Marine Information Science and Technology, Ocean College, Zhejiang University, Zhoushan, CN
2 Zhejiang Ocean University, Zhoushan, CN
E-mail: mail_zhaohan@zju.edu.cn

Abstract. In order to solve the problems of passive detection of very-low-frequency (VLF) underwater sound sources, this paper proposes a method of estimating sound source distance based on combining underwater sound field and Scholte wave field. VLF sources near the ocean bottom generate the sound field in the water, then seismic waves are excited by the of near-field effect. The surface wave propagating along the ocean bottom interface is the Scholte wave. By deploying a hydroacoustic&seismic-wave joint detection system on the ocean bottom, the acoustic field and the Scholte wave field excited by the source can be collected. Due to the different physical properties of water acoustics and Scholte waves, the Scholte waves can be distinguished by analysing the polarization characteristics of the captured signals. Due to the different velocity between the underwater acoustics and Scholte waves, the propagation delays to the joint detection system are also different, and the delay difference can be obtained by the correlation method. Combined with the surrounding parameters, the distance of the target source can be determined. Theoretical analysis and finite element simulation experiments show that this method can estimate the position information of near-ocean-bottom VLF underwater sources in the ideal case.

1. Introduction

The stealth technology of modern underwater sound sources has greatly reduced the level of high- and mid-frequency noise compared to the past. At present, the underwater target radiation noise mainly concentrates on the low-frequency and very-low frequency bands. The passive ranging of underwater targets, as the main task of the underwater detection system, has always been a hot and difficult problem in the research of underwater acoustics [1-3]. At present, there are mainly 3 kinds of passive ranging technologies, namely passive array ranging from three-element array, passive ranging from focused beamforming and passive ranging from matching fields. Each of these methods uses a plurality of sub-arrays with very long intervals to measure the azimuth angle or measure the curvature of the wavefront to obtain the distance of the target sound source. For a VLF underwater acoustic field, if a half-wavelength array is used, the array element spacing needs to reach tens of meters. These methods have extremely high requirements for the accuracy of time-measurement and array element arrangement. In engineering, it is not ideal to achieve very low frequency sound source ranging through sonar arrays.

From the 1940s to the present, many researchers have done a series of studies on low-frequency and very-low-frequency sound propagation in the sea. These studies use OBS and hydrophones. In 1947, Scholte [4] discovered a kind of interface waves between solid and liquid that is now called the

Scholte wave. In 1980, Dieter Rauch et al. [5] conducted an underwater experiment for the reception of ocean bottom seismic waves caused by explosion. The time-distance signals, dispersion analysis diagrams, attenuation curves, and particle motion trajectories of seismic waves were obtained, and the characteristics of Scholte waves were summarized. In 2012, Bing Yan et al. [6] of Naval University of Engineering used a single OBS to estimate the target's parameters and obtain the DOA estimation, which is independent with distance.

Over the years, people have made considerable efforts in the interface-wave measurement and inversion for ocean acoustics applications [7-10]. On the other hand, people have made considerable progress in the application of ocean bottom seismometers and acoustic vector sensors for underwater target detection [11-14].

In this paper, a new method for distance estimation of VLF sound sources near the ocean bottom is proposed by obtaining the delay difference between different waveguides which are acoustics and Scholte waves.

2. Signal model and ranging method

2.1. Ocean Bottom Sound Field Analysis

The ocean bottom is the interface between seawater (liquid) and sediment (solid). Scholte waves exist at the solid-liquid interface. Scholte waves' amplitudes decrease exponentially with increasing distance from the interface. Scholte waves have the following properties:

- Its propagation speed is approximately 90% of the shear wave speed.
- Its particle movement trace is rotational.
- It is dispersive when the shear speed varies with depth.

2.1.1. Velocity of Scholte waves. When the solid medium is a homogeneous and isotropic half infinite space, and the liquid medium is homogeneous, isotropic, with finite depth, the formula for the phase velocity of the Scholte wave is as follows [15]:

$$4\left[1-\left(\frac{v_{\mathrm{p}}}{c_{\mathrm{p1}}}\right)^2\right]^{1/2}\left[1-\left(\frac{v_{\mathrm{p}}}{c_{\mathrm{s1}}}\right)^2\right]^{1/2}-\left(2-\frac{v_{\mathrm{p}}^2}{c_{\mathrm{s1}}^2}\right) \tag{1}$$

$$=\frac{\rho_0}{\rho_1}\left(\frac{v_{\mathrm{p}}}{c_{\mathrm{s1}}}\right)^4\left[1-\left(\frac{v_{\mathrm{p}}}{c_{\mathrm{p1}}}\right)^2\right]^{1/2}\left[1-\left(\frac{v_{\mathrm{p}}}{c_{\mathrm{p0}}}\right)^2\right]^{-1/2}\tanh\{\frac{\omega D}{v_{\mathrm{p}}}\left[1-\left(\frac{v_{\mathrm{p}}}{c_{\mathrm{p0}}}\right)^2\right]^{1/2}\}$$

Equation (1) is the dispersion equation for the case with finite water depth. Where the liquid has the sound speed c_{p0} and density ρ_0. And the solid medium has P- and S- wave speeds c_{p1} and c_{s1}, and its density is ρ_1. D is the water depth. When $D \to 0$, this expression becomes Reileigh wave formula. When $D \to \infty$, this expression becomes identical to the expression of equation for the infinite water depth. Equation (1) has always one positive real root, which is the Scholte wave $v_{\mathrm{p}} = v_{\mathrm{sch}}$ and can be found numerically.

The group speed v_{g} of Scholte wave can be found by differentiation - that is, by taking the derivative - and is expressed as

$$\frac{v_{\mathrm{p}}}{c_{\mathrm{p1}}}=\frac{\mathrm{d}\omega}{\mathrm{d}k}=\frac{v_{\mathrm{p}}}{1-\frac{\omega}{v_{\mathrm{p}}}\frac{\mathrm{d}v_{\mathrm{p}}}{\mathrm{d}\omega}} \tag{2}$$

2.1.2. Polarization properties of Scholte waves. The components of the particle displacement vector of the Scholte wave is given as follows.

The displacement components in the water are expressed as

$$u_{\mathrm{x0}}=u_{\mathrm{x0}}(k,z)\sin(kx-\omega t),(z\le 0) \tag{3}$$

$$u_{z0} = u_{z0}(k,z)\cos(kx-\omega t),(z\le 0) \tag{4}$$

where

$$u_{x0}(k,z) = -kA\exp(\alpha_{p0}z) \tag{5}$$

$$u_{z0}(k,z) = -\alpha_{p0}\exp(\alpha_{p0}z) \tag{6}$$

The displacement components in the bottom are expressed as

$$u_{x1} = u_{x1}(k,z)\sin(kx-\omega t),(z\ge 0) \tag{7}$$

$$u_{z1} = u_{z1}(k,z)\cos(kx-\omega t),(z\ge 0) \tag{8}$$

where

$$u_{x1}(k,z) = \frac{\alpha_{p0}kA}{\kappa_{s1}^2\alpha_{p1}}\{2\alpha_{p1}\alpha_{s1}\exp(-\alpha_{s1}z)-(k^2+\alpha_{s1}^2)\exp(-\alpha_{p1}z)\} \tag{9}$$

$$u_{z1}(k,z) = \frac{\alpha_{p0}A}{\kappa_{s1}^2}\{2k^2\exp(-\alpha_{s1}z)-(k^2+\alpha_{s1}^2)\exp(-\alpha_{p1}z)\} \tag{10}$$

Equations (3) - (10) are parametric representations of ellipses having their main axes parallel to axes of the coordinate system. Where A is Scalar displacement potential amplitude of the water. Since the horizontal wave number, k, is the same for all waves at the interface, the vertical wave numbers describing the vertical decays of the fields have to be

$$\alpha_{p0} = (k^2-\kappa_{p0}^2)^{1/2} \tag{11}$$

$$\alpha_{p1} = (k^2-\kappa_{p1}^2)^{1/2} \tag{12}$$

$$\alpha_{s1} = (k^2-\kappa_{s1}^2)^{1/2} \tag{13}$$

where

$$k = \frac{\omega}{v_p},\kappa_{p0} = \frac{\omega}{c_{p0}},\kappa_{p1} = \frac{\omega}{c_{p1}},\kappa_{s1} = \frac{\omega}{c_{s1}} \tag{14}$$

With increasing distance from the interface, the displacement amplitudes $\hat{u}_{x0}$, $\hat{u}_{z0}$ and $\hat{u}_{z1}$ decrease exponentially without changing sign. The horizontal displacement in the bottom, $\hat{u}_{x1}$, shows the same asymptotic behavior, but with the sign changing at the depth of about one-tenth of the Scholte wavelength. The penetration depth in the water is about one-half of the Scholte wavelength. In liquid, the eccentricity of the displacement elliptical trajectory is close to 0, and the trajectory is close to a circle. In the sediment layer, the ellipse is elongated and the amplitude of the displacement vertical component is greater, i.e. $|\hat{u}_{z1}|>|\hat{u}_{x1}|$. The interface waves are confined to a narrow stratum close to the interface, which means that they have cylindrical propagation loss (i.e., $1/r$) rather than spherical spreading loss (i.e., $1/r^2$). Cylindrical spreading loss indicates that, once an interface wave is excited, it is likely to dominate other waves that experience spherical spreading at long distances.

The interface waves can be excited by a point source close to the interface, that is, as a near-field effect.

2.1.3. Dispersion of Scholte waves. When the shear speed in the bottom varies with depth, the velocity of Scholte waves is not a constant. This is due to the fact that the Scholte wave is related to the shear wave velocity of solid media, while the Scholte wave penetration depth is different for different frequencies. The dispersion properties of the Scholte wave can be expressed by the dynamic stiffness matrix approach [16]. The frequency band most concerned in this study is 30-50Hz and the dispersion of Scholte wave in this band is not distinct. Therefore, this study takes the ideal condition assumption that the Scholte wave velocity does not change with frequency.

2.2. Distance Estimation

Since underwater acoustics and Scholte waves have different velocities, the propagation delays to the joint detection system are also different. The delay difference can be obtained, and the distance of the target source can be determined by combining with the surrounding parameters.

A VLF hydroacoustic&seismic-wave joint detection system is deployed on the ocean bottom in order to capture underwater acoustics and ocean bottom Scholte waves. The join detection system consists of an acoustic vector sensor (AVS) and an ocean bottom seismometer (OBS). An AVS is able to measure both the acoustic pressure and the three particle velocity components providing an estimate of the full directional acoustic intensity field. An OBS is able to measure the three particle velocity of ocean bottom. By analyzing the signals captured by the joint detection system, the delay difference information for the two types of wavefields can be obtained.

2.2.1. Distinction of acoustics and Scholte waves. According to 2.1.2, the particle displacement track of Scholte wave in the sediment layer is elliptical and the vertical component is greater, i.e. $|\hat{u}_{z1}|>|\hat{u}_{x1}|$. Scholte waves can be detected based on this feature.

2.2.2. Determination of delay difference. In this study, the delay difference of 2 types of waves is the core. The accuracy of delay difference estimation determines the accuracy of ranging. This paper uses classic cross-correlation method to find the delay difference. This method obtains the correlation peak coordinate value as the delay difference by the cross correlation function of the two signals. The advantages of this method are that it can not only solve the delay difference, but also detect the correlation of different signals. This ensures the measured waves are from the same source via different channels.

Let the signal emitted by the sound source in the water be $s(t)$. The received signal of sound pressure channel of the AVS is $r_{\mathrm{p}}(t)$, and the received signal of vertical velocity channel of the OBS is $r_{\mathrm{v}}(t)$. So

$$r_{\mathrm{p}}(t) = a_1(t)s(t-\tau_{\mathrm{w}}) + a_2(t)s(t-\tau_{\mathrm{sch}}) + n_{\mathrm{p}}(t) \tag{15}$$

$$r_{\mathrm{v}}(t) = a_3(t)s(t-\tau_{\mathrm{w}}) + a_4(t)s(t-\tau_{\mathrm{sch}}) + n_{\mathrm{v}}(t) \tag{16}$$

where τ_{w} is the acoustics delay, τ_{sch} is the Scholte wave delay. $n_{\mathrm{p}}(t)$, $n_{\mathrm{v}}(t)$ are noise. $a_1(t)$, $a_2(t)$, $a_3(t)$, $a_4(t)$ are distortions of signals. It is assumed here that they are time invariant, denoted by a_1, a_2, a_3, a_4. In the sound pressure channel of AVS, the direct acoustics signal in the water accounts for a large proportion; in the vertical velocity channel, the Scholte waves signal in the bottom accounts for a large proportion. Which can be recorded as

$$\frac{a_1}{a_2} > \frac{a_3}{a_4} \tag{17}$$

The cross-correlation function of $r_{\mathrm{p}}(t)$ and $r_{\mathrm{v}}(t)$ is denoted as $R_{\mathrm{p,v}}(\tau)$. The delay difference estimate tau can be obtained from coordinates of the correlation peak of the cross-correlation function. For real signals, the cross-correlation function is defined as

$$R_{\mathrm{p,v}}(\tau) = \int_{-\infty}^{+\infty} r_{\mathrm{p}}(t-\tau)r_v(t)\mathrm{d}t = \int_{-\infty}^{+\infty} r_{\mathrm{p}}(t)r_v(t+\tau)\mathrm{d}t \tag{18}$$

Here assumes that $n_{\mathrm{p}}(t)$, $n_{\mathrm{v}}(t)$ is Gaussian white noise, has no correlation with itself, and is uncorrelated with the source signal, so it can be ignored. Substituting equation (15) and equation (16) into equation (18) yields

$$R_{\mathrm{p,v}}(\tau) = (a_1a_3 + a_2a_4)R_{\mathrm{s}}(\tau) + a_1a_4R_{\mathrm{s}}(\tau - \tau_{\mathrm{sch}} + \tau_{\mathrm{w}}) + a_1a_3R_{\mathrm{s}}(\tau + \tau_{\mathrm{sch}} - \tau_{\mathrm{w}}) \tag{19}$$

where $R_{\mathrm{s}}(\tau)$ represents the autocorrelation function of $s(t)$. The peak of the autocorrelation function is taken at the origin. Therefore when $\tau = \tau_{\mathrm{sch}} - \tau_{\mathrm{w}}$, $R_{\mathrm{p,v}}(\tau)$ has a clear peak. Symmetrically along the y-axis, when $\tau = -(\tau_{\mathrm{sch}} - \tau_{\mathrm{w}})$, $R_{\mathrm{p,v}}(\tau)$ has another peak. $a_1a_4 > a_2a_3$ is known from inequality (17), so the peak at $\tau = \tau_{\mathrm{sch}} - \tau_{\mathrm{w}}$ is higher. In the ideal case, the delay difference derived from the peak coordinate is the delay difference of waves over the different channels to the receiver. That is, the delay difference between the direct acoustics and ocean bottom Scholte waves.

$$\hat{\tau} = \arg\max_{\tau} R_{\mathrm{p,v}}(\tau) \qquad \text{s.t.} \quad \tau > \varepsilon \tag{20}$$

Where $\hat{\tau}$ is the delay difference estimate and ε is the time delay for the value of the cross-correlation function to decrease to noise level near zero.

2.2.3. Ranging by delay difference. We consider the situation depicted in figure 1, where the distance from the source to the bottom is *D*, and the horizontal distance from the source to the receiver is *L*.

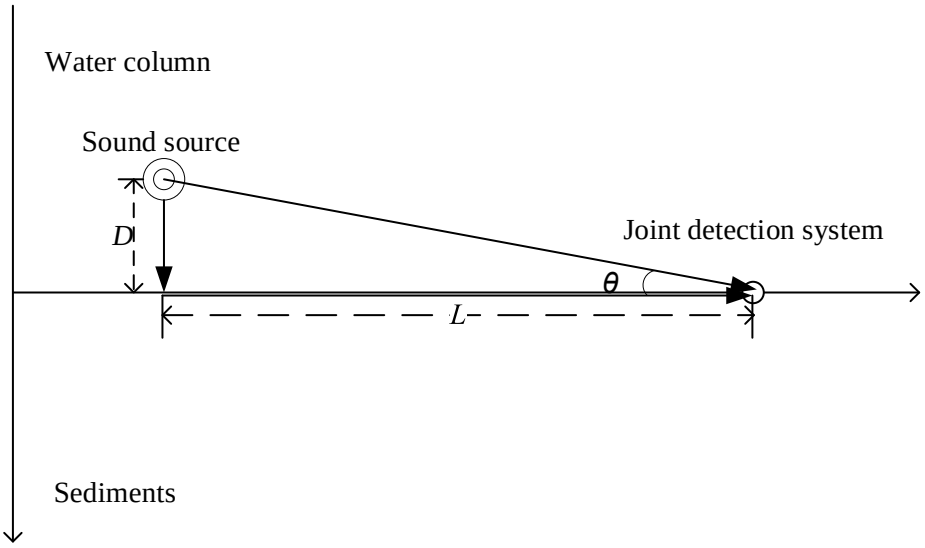

Figure 1. Wave propagation model.

Assuming that the water column and sediments are homogeneous isotropic media, then the delays for the propagation of the signals from the sound source through the direct acoustics in the water and the Scholte wave on the ocean bottom to the joint detection system are

$$\tau_{\mathrm{w}} = \frac{(D^2 + L^2)^{1/2}}{c_{\mathrm{p0}}} \tag{21}$$

$$\tau_{\mathrm{sch}} = \frac{D}{c_{\mathrm{p0}}} + \frac{L}{v_{\mathrm{sch}}} \tag{22}$$

Delay difference can be obtained by the difference between equation (21) and equation (22)

$$\tau = \frac{D}{c_{\mathrm{p0}}} + \frac{L}{v_{\mathrm{sch}}} - \frac{(D^2 + L^2)^{1/2}}{c_{\mathrm{p0}}} \tag{23}$$

Because the sound source is very close to the bottom, *D* is small. The effective range of detection is much greater than the distance from the source to the bottom, i.e. $L \gg D$. The acoustic speed in the water is greater than the shear wave velocity of the sediments and larger than the Scholte wave velocity, i.e. $c_{\mathrm{p0}} > v_{\mathrm{sch}}$. Therefore, $L/v_{\mathrm{sch}} \gg D/c_{\mathrm{p0}}$. And because $\theta \to 0$, $\cos\theta \to 1$, $\left(D^2+L^2\right)^{1/2} \to L$. So equation (23) can be simplified as

$$\tau = \frac{L}{v_{\mathrm{sch}}} - \frac{L}{c_{\mathrm{p0}}} \tag{24}$$

and then

$$\hat{L} = \hat{\tau} \cdot \frac{c_{\mathrm{p0}} \cdot v_{\mathrm{sch}}}{c_{\mathrm{p0}} - v_{\mathrm{sch}}} \tag{25}$$

Equation (25) is the distance estimation equation obtained by the delay difference.

3. Simulation Experiment and Model Validation

Finite element method (FEM) is one of the effective methods of sound field modeling. Especially when it involves multiple physical fields, FEM can co-process the coupling conditions of each physical field. This paper uses FEM to model and simulate the ocean bottom environment.

3.1. Model Parameter Settings

3.1.1. Surroundings parameters. The ocean bottom environment model parameters are set as table 1:

Table 1. Properties of the water column and sediment used to model.

Medium	Layer thickness (m)	c_p (ms^{-1})	c_s (ms^{-1})	ρ (kg m^{-2})
Water	20	1500	-	1000
Sediment				
Layer 1	50	2500	400	2000
Layer 2	200	3000	550	2500

3.1.2. Sound source information. A VLF sound source in water is placed 1m from the ocean bottom to excite water acoustics and Scholte waves, i.e. $D = 1$.
The source signal is

$$s(t) = \frac{1000}{\pi} \cdot \mathrm{sinc}(\frac{10}{\pi} t) \cdot \mathrm{e}^{\mathrm{j}40t} \tag{26}$$

By the Fourier transform, the above equation is converted into the frequency domain form

$$S(f) = \begin{cases} 100, & 30 \le f \le 50 \\ 0, & \text{other} \end{cases} \tag{27}$$

3.1.3. Capture position. The capture position in the water is placed at a distance of 0.5m from the bottom. The capture position under the bottom is placed at a distance of 0.1m from the bottom. This is consistent with existing joint detection system.
The horizontal distance from the sound source to the capture position is from 0m to 5000m, every 10m, i.e. $L = 0, 10, 20, \ldots, 5000$.

3.2. Distance Estimation Results

From time 0, collect 16 seconds of signals. The receiving signals of the water acoustic pressure channel and the vertical component of sediment particle velocity channel are shown in figure 2.

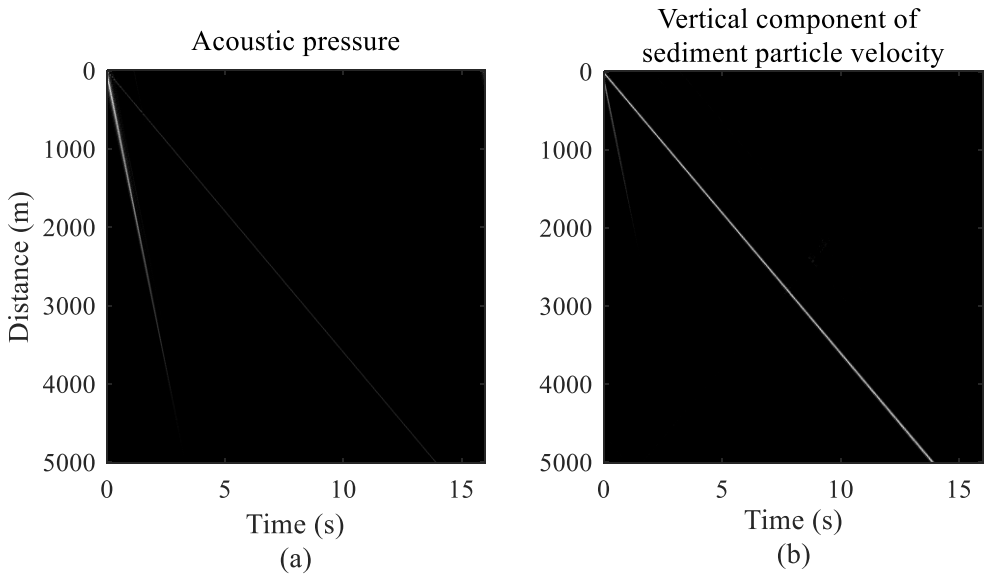

Figure 2. The intensities vary with time and distance.

In figure 2, the lighter the color, the greater the intensity. In both (a) and (b), faster wave (left line) is direct underwater acoustics, and the slow wave (right line) is ocean bottom Scholte wave. In the acoustic pressure channel, the direct underwater acoustics is stronger; in the vertical velocity channel,

the Scholte wave is stronger. It can also be seen that the Scholte wave attenuation is smaller than acoustics over long distances.

The signals of the two channels are extracted, and they are substituted into equation (20) to calculate the delay difference of direct underwater acoustics and ocean bottom Scholte wave. And then the distance can be obtained by equation (25). Some of distance estimation results are shown in table 2, figure 3 and figure 4.

Table 2. The results of delay difference and estimated distance.

Actual distance(m)	Delay difference(s)	Estimated distance(m)	Error (m)	Actual distance(m)	Delay difference(s)	Estimated distance(m)	Error (m)
100	0.209	98.32	1.68	2000	4.227	1987.78	12.22
500	1.064	500.15	-0.15	3000	6.345	2983.81	16.19
1000	2.109	991.75	8.25	4000	8.464	3979.84	20.16
1500	3.182	1496.18	3.82	5000	10.6	4984.41	15.59

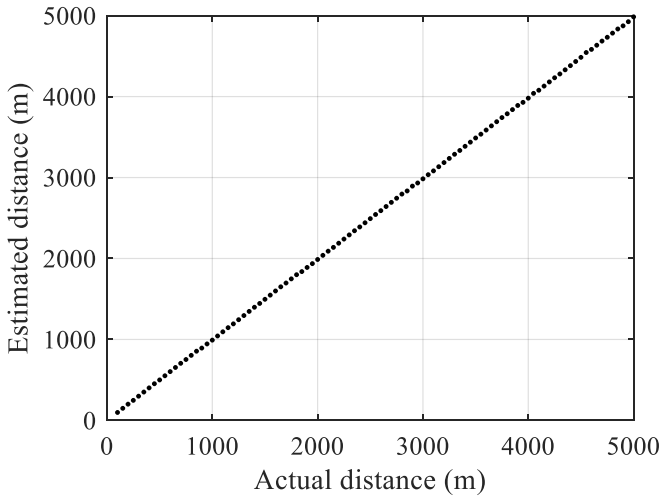

Figure 3. Estimated distance compared to actual distance.

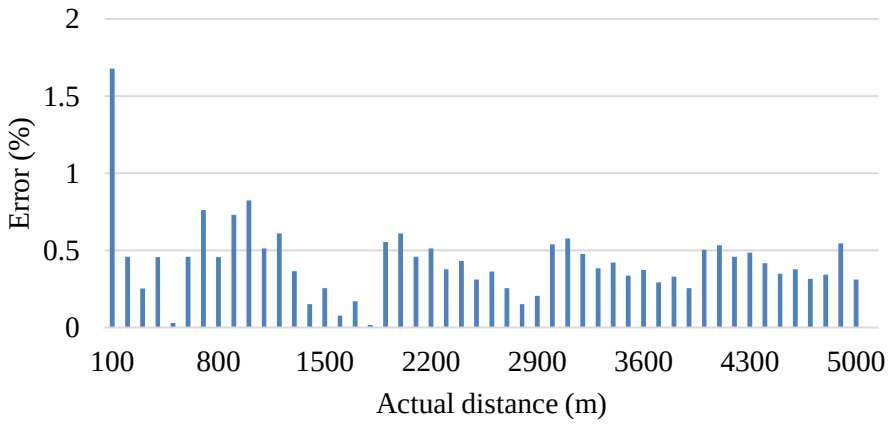

Figure 4. Ranging error ratio.

4. Conclusion

This paper proposes a distance estimation method for VLF sound sources near the ocean bottom. The method simultaneously measures underwater acoustics and ocean bottom Scholte waves, uses the delay difference of the two channels, and combines the parameters of ocean bottom surroundings to estimate the distance.

Under ideal simulation conditions, when the range is from 100m to 5000m, the range error does not exceed 2%.

This method does not require the deployment of sonar arrays as in the traditional method. It is only necessary to deploy an AVS-OBS joint detection system on the ocean bottom. The difficulty in engineering is greatly reduced.

A single AVS has the ability to estimate the DOA of the sound source, but cannot estimate the distance. By combining underwater acoustics and Scholte waves, the distance information can be obtained. Combining the distance and the DOA, the complete position information of the target sound source can be obtained.

5. References

[1] Qihu L I 2015 A new method of passive ranging for underwater target: distance information extraction based on waveguide invariant *Chinese Journal of Acoustics* 34 97-106

[2] Annabattula J, Rao S K, Murthy A S D, Srikanth K S and Das R P 2015 Underwater passive target tracking in constrained environment *Indian Journal of Science and Technology* 8

[3] Song X, Zhao A and Li M 2017 Passive ranging technique using waveguide invariant in shallow water with thermocline *J SYST ENG ELECTRON* 28 244-50

[4] Scholte J G 1947 The range of existence of Rayleigh and Stoneley waves *GEOPHYS J INT* 5 120

[5] Rauch D 1980 Seismic interface waves in coastal waters: A review *Seismic Interface Waves in Coastal Waters A Review*

[6] Yan B, Guo H, Li X and Yu D 2012 Moving target parameter estimation based on single seismometer *Journal of Naval University of Engineering* 24 66-70

[7] Godin O A and Chapman D M F 2001 Dispersion of interface waves in sediments with power-law shear speed profiles. I. Exact and approximate analytical results *J ACOUST SOC AM* 110 1890-1907

[8] Chapman D M F and Godin O A 2001 Dispersion of interface waves in sediments with power-law shear speed profiles. II. Experimental observations and seismo-acoustic inversions *J ACOUST SOC AM* 110 1908

[9] Dong H, Allouche N, Drijkoningen G G and Versteeg W 2010 Estimation of Shear-Wave Velocity in Shallow Marine Environment *Proc. of the 10th European Conference on Underwater Acoustics* (Istanbul) pp 175-180

[10] Dong H, Hovem J M and Frivik S A 2015 Estimation of shear wave velocity in seafloor sediment by seismo-acoustic interface waves: a case study for geotechnical application. *Theoretical and Computational Acoustics* (Hangzhou) pp 33-43

[11] Kalgan A, Bahl R and Kumar A 2015 Source ranging and direction of arrival estimation using accelerometer based implementation of prototype acoustic vector sensor. In: *Underwater Technology* (Chennai: IEEE) pp 1-6

[12] Widmaier M, Fromyr E and Dirks V 2015 Dual-sensor towed streamer: From concept to fleet-wide technology platform *first break* 33 83-9

[13] Felisberto P, Santos P, Maslov D and Jesus S M 2016 Combining pressure and particle velocity sensors for seismic processing. In: *OCEANS 2016 MTS/IEEE* (Monterey: IEEE) pp 1-6

[14] Song X, Zhao A and Li M 2017 Passive ranging technique using waveguide invariant in shallow water with thermocline *J SYST ENG ELECTRON* 28 244-50

[15] Dong H and Hovem J M 2011 *Interface Waves, Waves in Fluids and Solids* (London: InTech) pp 153-176

[16] Potty G R and Miller J H 2012 Measurement and modeling of Scholte wave dispersion in coastal waters *AIP Conference Proceedings* (New York: AIP) pp 500-507